DIFFERENTIAL RADIODIAGNOSIS OF SALIVARY GLAND MASSES

UDC 616.316–006–079.4
Received 17.05.2013

© **E.A. Egorova,** D.Med.Sc., Professor, the Department of Radiology[1];
M.V. Smyslenova, D.Med.Sc., Professor, the Department of Radiology[1];
N.P. Obinya, PhD, Dental Surgeon[2];
D.K. Faskhutdinov, Tutor, the Department of Departmental Dental Surgery[1]

[1]Moscow State University of Medicine and Dentistry named after A.I. Evdokimov, Delegatskaya St., 20/1, Moscow, Russian Federation, 127473;
[2]City Polyclinic No.175, Chelyabinskaya St., 16, Moscow, Russian Federation, 127206

The aim of the investigation was to evaluate the possibilities of radiological methods in differential diagnostics of salivary gland masses.

Materials and Methods. 76 patients with tumors and tumor-like salivary gland masses were examined. We analyzed the findings of their physical examination, and performed operative interventions compared to the data of histological verification, multiplanar reconstruction sialography and ultrasound investigation.

Results. At clinical examination the symptoms were non-specific. 97.5% of patients presented with a constant mass in the affected salivary gland. in 14.5% of patients the mass grew during the last 3–4 months; and in 2.5% of patients it was an incidental finding and had no manifestations. The mostly involved glands (96% of cases) were parotid and submaxillary salivary glands. Tumor-like masses were found in 16 patients (21%), benign tumors — in 57 (75.0%), malignancies and locally destructive tumors — in 3 (4.0%).

Conclusion. High resolution ultrasound is the primary diagnostic technique of neoplastic masses of major salivary glands, and allows a reliable evaluation of the mass localization, shape, size, structure, borders, and vascularisation. Multiplanar reconstruction sialography enables to assess more precisely anatomical localisation of tumors and tumor-like masses of salivary glands with duct system, adjacent bone and soft tissue structures.

Key words: salivary glands; tumours; tumour-like masses; multiplanar reconstruction sialography; ultrasound investigation.

Neoplastic processes of major salivary glands (SG) contributes to about 1–2% of all tumors. This includes tumor-like masses, primary benign and malignant tumors. The peak incidence was recorded in middle-aged people (40–60 years). Male-female ratio is almost equal. Parotid and submandibular SG diseases are the most frequent. Neoplastic processes in sublingual and minor SG were rarely recorded. Malignant SG tumors metastasize in regional superficial and deep lymphatic nodes of the neck, though hematogenous spread to bones, lungs, brain, liver, etc is also possible [1–3].

Differential diagnosis of SG tumor and tumor-like diseases with inflammatory processes and vascular masses of this localization is a challenge [4–6].

Modern diagnostic techniques including ultrasound (US) and computed tomography (CT) sialography are now extensively used to study SG topography, function and pathological changes of parenchyma and ductal system. These techniques enable to obtain the required qualitative and quantitative imaging characteristics, and offer new possibilities for differential diagnosis of various SG pathological conditions.

The aim of the investigation was to evaluate the possibilities and role of multiplanar reconstruction sialography in differential diagnostics of salivary gland masses.

Materials and Methods. 76 patients with different SG masses were analyzed. The patients were examined taking into consideration the simptomatology, history, the findings of their physical and radiological examinations including US (n=31; 40.8%) and multidetector CT sialography (n=76; 100%).

US was performed on ultrasound device iU-22 (Philips, Holland) using linear array transducers (working frequency range: 5–17 MHz). The patients were examined in B-mode, with color Doppler and energy mapping, pulse wave Doppler. Symetrical cervical and facial zones were examined, as well as multiple view scanning of areas of interest.

Multidetector CT sialography was performed on Brilliance-64 (Philips, Holland) tomography in two stages:

For contacts: Obinya Nicolay Pavlovich, phone: +7 926-210-32-13; e-mail: mio_veter@mail.ru

native examination (with comparative assessment of the shape, size, borders and density of the studied gland with a contralateral SG on symmetrical areas);

contrast enhancement of a ductal system of the studied SG (according to a modified technique of I.F. Romacheva et al., 1987) was followed by the administration of iodine containing radiopaque contrast agent (320–350 mg I/mL) to the extent of 2–3 mL using a plastic catheter, 0.6 mm in diameter, through the excretory duct of the gland.

I.F. Romacheva scheme (1973) was used in the assessment of multidetector CT sialography picture on axial sections, in multiplanar and three-dimensional (3D) reconstructions.

The analysis of the findings included:

the filling quality of the SG excretory duct (uniformity, contour, diameter (narrowing/ectasia), filling defect and contrast depot);

the presence of filling defects or cavities (a contrast agent depot) of ductal system in the area of SG parenchyma;

topographic and anatomical characteristics of SG masses in relation to other structures (tongue, muscles, teeth, jaws, etc).

Morphological study of biopsy or surgical material was performed in all cases of SG masses to determine the nature of the process.

Results and Discussion

Clinicopathologic characteristic of SG masses

1. Clinically — the simptomatology was non-specific. 97.5% of cases were distinguished by the presence of a constant mass in the affected SG, which expanded over the last 3–4 months in 14.5% of patients. In 2.5% of cases a SG mass was an incidental finding and had no manifestation. There were predominantly (96%) involved parotid SG (PSG) and submandibular SG (SMSG), sublingual SG (SLSG) masses were found in 4% of cases.

Visual examination of all patients with SG tumors and tumor-like masses revealed no skin changes. There was swelling of various degrees depending on the mass size. 27 patients (35.5%) had tenderness on palpation, 10 (13%) — enlargement and slight tenderness of the regional lymph nodes and palatine tonsils.

SG masses had no specific clinical signs, and could be differentiated only by the comparison of the findings of radiological methods and morphological verification.

2. Morphological type of the masses corresponded to:

tumor-like masses (n=16; 21%), among them 2 (2.5%) cases were diagnosed as Stafne pseudocysts — a result of SMSG accessory lobule ectopia into the mandible, 3 (4%) cases — retention cysts developed from SLSG ducts and lobules — ranulas, the rest 11 (14.5%) cases had the cysts located in SG parenchymal part;

benign tumors (n=57; 76.5%), among them pleomorphic adenomas were the most common (n=48; 63.3%) characterized by a variety and heterogenicity of structure, and containing epithelial and mesenchymal components, lipomas were diagnosed in 7 (9.2%) cases due to SG fatty hyperplasia (in Madelung's disease as well), teratodermoids of the mouth floor were found in 2 (2.5%) patients;

malignant locally destructive tumors (n=3; 4%) in the form of stage I acinic cell carcinomas (T_1), which did not exceed 2.0 cm in its maximum dimension, were located in the gland parenchyma, did not spread beyond the capsule, and consisted of basophil cells resembling albuminous cells of the gland acinus.

Comparison of clinical findings, the results of morphological verification and multiplanar reconstruction sialography

1. Tumor-like masses.

Ranulas (n=3; 4%) were located under the tongue, in the anterior part of the mouth floor, had heavy elastic consistency, the mucosa above them was flexible, thin, cyanotic. There were no reactive changes of the surrounding tissues and regional lymph nodes. Morphological study of ranulas revealed connective tissue of various maturity degrees (fibrous, granulation), its bounaries penetrating the connective tissue interlayers of SLSG lobules.

On native tomograms a mass was not differentiated from anatomical structures of the mouth floor (Fig. 1, *a*). Multidetector CT sialography with multiplanar and 3D-reconstructions (Fig. 2, *b, c*) enabled to obtain reliable diagnostic information and detect in 2 patients (2.6%) — one cystic cavity and in 1 patient (1.3%) — two cystic cavities connected among themselves by a fistula (n=1; 1.3%).

Stafne pseudocysts (n=2; 2.5%) represented a dystopic accessory SG lobule (submandibular SG, rarely — sublingual SG) in the mandible with the surrounding bone depressed, with a cortical defect on oral side. They were incidental findings and had no clinical manifestations.

Native multidetector CT showed bone defects reaching 0.5–1.5 cm, of round shape, with sclerotic margins, containing the components of liquid and fat density. Sialograms demonstrated a contrast invariable ductal

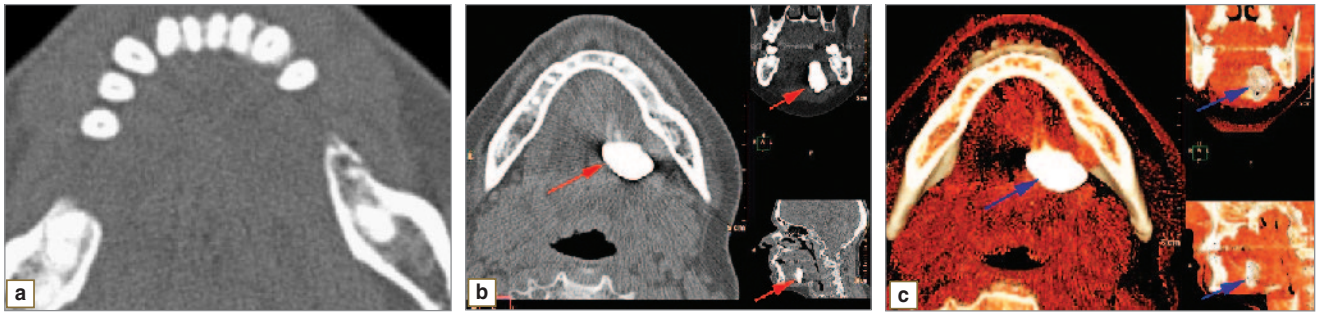

Fig. 1. Multidetector CT images: *a* — native investigation, axial section; *b* — sialogram, multiplanar reconstruction; *c* — sialogram, 3D-reconstruction, show ranula (a cavity with clear contours) after SLSG ductal system contrast enhancement (arrows)

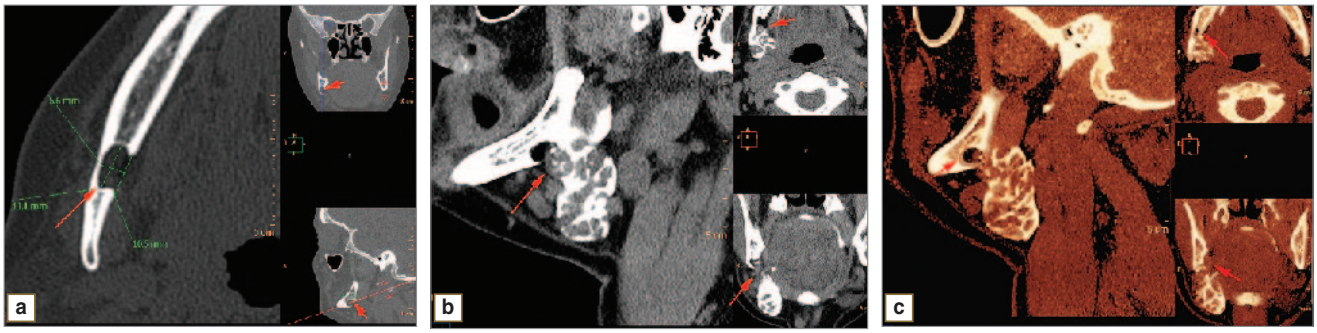

Fig. 2. Multidetector CT images: *a* — native investigation, multiplanar reconstruction; *b* — sialogram, multiplanar reconstruction; *c* — sialogram, 3D- reconstruction, demonstrate cortical defect of the mandibular body on the right oral side due to the depression of osseous tissue by SMSG accessory lobule (arrows)

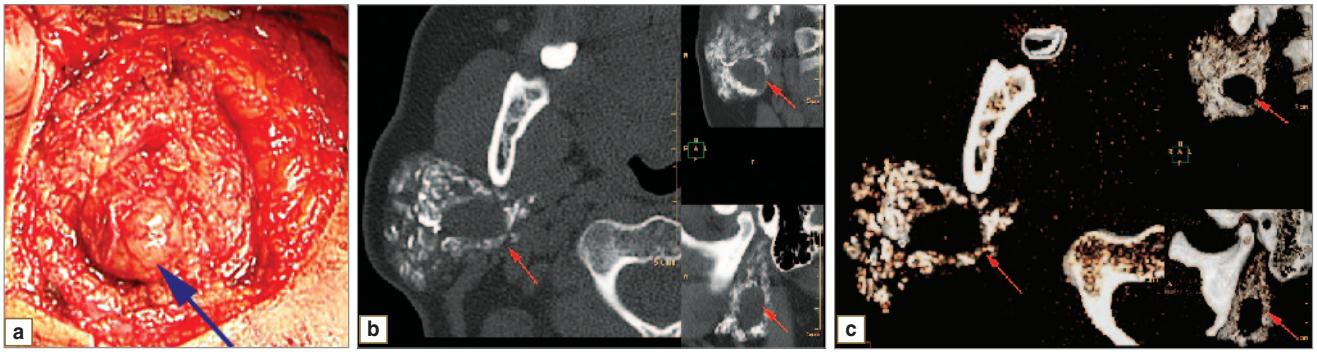

Fig. 3. The comparison results of intraoperative picture of the cyst and multidetector CT sialography in the right PSG contrast enhancement. The presented an intraoperative image of the mass *(a)* and multidetector CT images (*b* — sialogram, multiplanar reconstruction; *c* — sialogram, 3D- reconstruction) show an oval liquid cavity in the lower pole of the gland, with clear margins, with the ducts observed at all levels, and displaced aside, forward and downward (arrows)

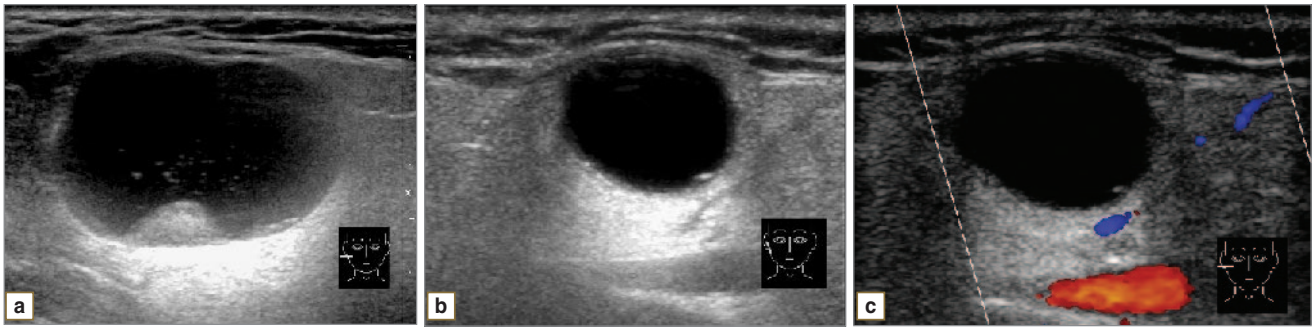

Fig. 4. Echograms of different SG cysts: *a* — B-mode, a cyst in the right PSG in the form of a liquid mass with a capsule and heterogeneous content; *b* — B-mode, a cyst is seen in the gland parenchyma in the form of homogeneous mass of liquid density, the flow in the cyst view in color Doppler *(c)* mapping is not revealed

system of the gland in the cavity of mandibular bone defects (Fig. 2, *a–c*).

Cysts (n=11; 14.5%) at parenchyma level were diagnosed most frequently (81.8%) in PSG. On palpation there were determined painless, non-mobile tumor-like masses of dense elastic consistency. There were revealed no skin changes above them and no reactions of regional lymph nodes.

Native multidetector CT showed 1.5–2-fold enlargement of the SG of interest compared to the contralateral side, its sharp borders differentiating against the background of surrounding fatty interlayers, fascias and muscles. The gland was heterogeneous due to the areas of soft tissue and liquid density. The cyst could be differentiated from the surrounding tissues using sialography, which enabled to visualize a mass of liquid density, of round or oval shape, with clear even borders at the level of one of the gland poles. Ductal system was observed at all levels, with no signs of duct ablation and deformity of ducts. Cysts caused dislocation of ducts pushing them aside, forward and downward (Fig. 3, *b, c*).

Ultrasound provided a more reliable diagnostic picture representing a cyst as a mass of liquid density, of homogeneous or heterogeneous structure due to the inclusions (cholesterol crystals), and surrounded by a capsule. All cysts were avascular, with no blood flow changes observed along the periphery (Fig. 4, *a–c*).

Cysts should be differentiated from cystic formations,

which are characterized by the cavities filled with fluid or heterogeneous content, in particular, by the presence of cystic cavity with a wall of ectopic derma with perspiratory and sebaceous glands, and containing a porridge-like mass of desquamated epidermis and cholesterol, and referred to ***dermoid cysts (teratodermoids).*** They can occur in various parts of maxillofacial area, and their preferred location is mouth floor, where they locate in between the mandibular internal surface and the hyoid bone. Most teratodermoids are benign, though sometimes can become malignant. Depending on a growth direction and topographo-anatomical locations, sublingual and submental cysts are distinguished. Clinically, they are solitary or, rarely, multiple expansively growing masses. Multidetector CT signs of dermoid cysts are characterized by the presence of a cystic cavity connected with the mandible or hyoid bone by an orifice. The content of a dermoid cyst is heterogeneous: fatty, fluid, or soft tissue. The surrounding structures appear dislocated at the mass level, and if cysts are large-sized, their atrophy due to pressure can occur (Fig. 5, *a–d*).

2. Benign tumors.

All benign tumors were characterized by scanty clinical presentation and expansive growth. Multidetector CT sialograms represented them as inclusions of soft tissue or fat density with clear boundaries. There were no ducts discontinued, the ducts being located to a greater or lesser degree depending on a tumor size. In large masses the surrounding SG parenchyma looked thin due to atrophy.

The most common tumors were ***pleomorphic adenomas*** (n=48; 63.3%) characterized by heterogeneous structure containing epithelial and mesenchymal components. On palpation adenomas were dense, painless, non-adherent with surrounding tissues. Skin integument above the adenomas was of usual color, there were no hyperplastic changes of regional lymph nodes.

On ultrasound, adenoma presented as a hypoechogenic mass, with smooth or irregular, but always clear margins, with a well differentiated capsule. The tumor structure was determined to be heterogeneous. In most cases Doppler US revealed the small diameter vessels with low-speed blood flow (up to 10–20 cm/s) along the mass periphery, or the absence of vascularization signs (Fig. 6, *a, b*).

Native examination and multidetector CT sialography showed the interested SG to be enlarged in size, with clear margins, and differentiated surrounding tissues. The adenoma was visualized as a soft tissue conglomerate deep in the gland or in one of the gland poles (Fig. 7*, a–c*).

7 patients (9.2%) were found to have non-epithelial benign masses consisting of fatty tissue — ***lipomas (sialolipomas).*** Their diagnosis was of no difficulty, since multidetector CT image was very specific: a well-delineated area of low, fat density with regular margins was seen against the background of SG parenchyma of liquid density (Fig. 8, *a–c*).

3. Malignant tumors.

Locally destructive acinic cell carcinomas of SG were found in 4% (n=3) of cases. All were women over 40. One

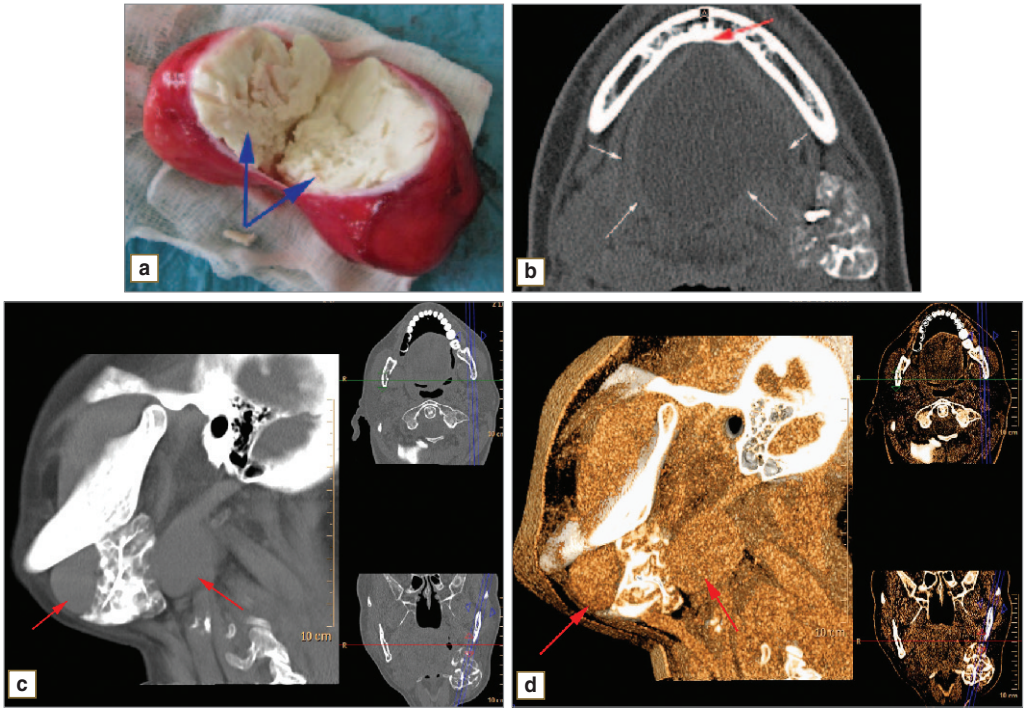

Fig. 5. The comparison results of intraoperative picture of a dermoid cyst of the mouth floor and multidetector CT sialography in the left SMSG ductal system contrast enhancement: the photograph of the mass excised during the surgery *(a)* and multidetector computer tomograms (*b* — sialogram, axial section; *c* — sialogram, multiplanar reconstruction; *d* — sialogram, 3D-reconstruction) show a cystic mass surrounded by a thin-walled capsule and filled by fatty content (white arrows), connected with the mandible by a narrow isthmus, closely attached to the left SMSG and pushing it to the outside and compressing in anterio-posterior direction. SG ductal system is uniformly filled with contrast medium, and not changed (red arrows)

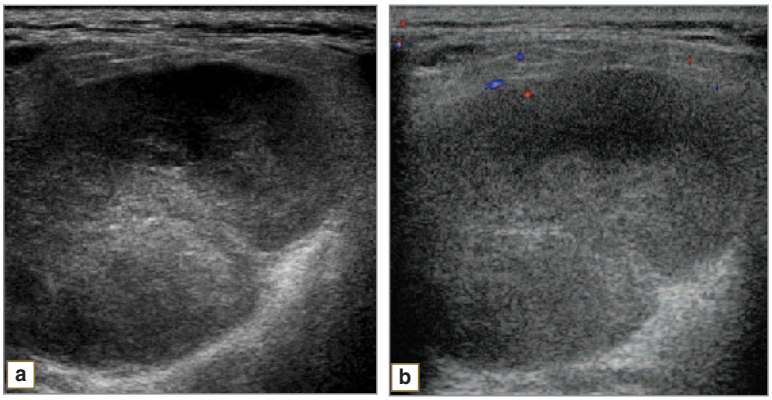

Fig. 6. Echograms of the left PSG: *a* — B-mode, pleomorphic adenoma in the form of a mass of reduced echogenicity, and moderately heterogeneous structure; *b* — color Doppler mapping, a single vessel along the adenoma capsule

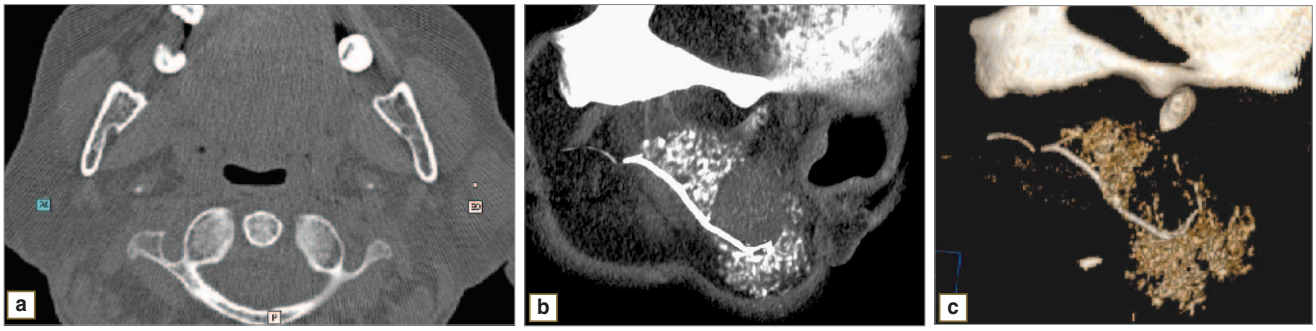

Fig. 7. Multidetector CT images: *a* — native investigation, axial section; *b* — sialogram, sagittal plane; *c* — sialogram, 3D-reconstruction, which demonstrate pleomorphic adenoma in the left PSG parenchyma, in the form of a soft tissue mass (density up to +69 HU) with a clear contour, the ducts are shown to be pushed aside and deformed and there is the parenchyma thinning at the adenoma level after the ductal system contrast enhancement

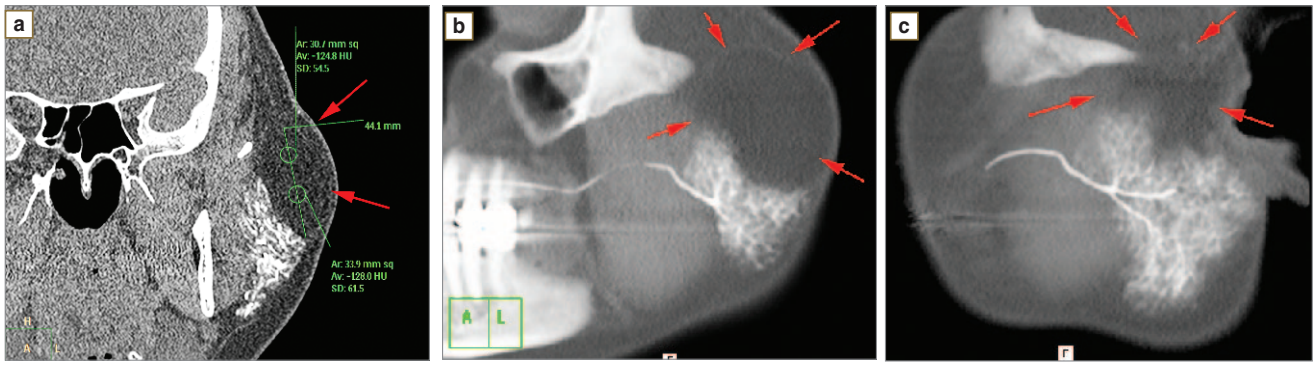

Fig. 8. Multidetector CT sialograms: *a* — frontal plane; *b* and *c* — a thick section in oblique planes, where the lipoma is seen in the left PSG parenchyma, in the form of a mass of fat density (from –130 to –120 HU) with a clear contour, which pushes the gland parenchyma downward, medially and forward

female patient was reliably found to have the malignization of pleomorphic adenoma. On palpation the tumor presented as a dense painless node with indistinct boundaries, there was observed the enlargement of regional lymph nodes (submandibular and cervical).

Ultrasound revealed in the gland an irregular-shaped mass of heterogeneous structure, with sharply reduced echogenicity. In all cases there was well determined a feeding vessel approaching a tumor node, the characteristic feature being the increase of a peripheral blood flow (over 30–40 cm/s). Two female patients had a high-degree vascularization of the tumor itself, and only one tumor had a moderate degree of blood supply (Fig. 9, *a–c*).

Computer tomograms showed the interested SG to be enlarged due to a heterogeneous mass (inside the tumor there were areas of liquid and soft tissue density), with irregular, and occasionally, indistinct boundaries. The changes of regional lymph nodes were assessed on multidetector CT images by analyzing their size, boundaries, shape, and the integrity of fat interlayers along the periphery. A round shape lymph node, the enlargement of the maximum size up to the level of over 0.8–1 cm, the heterogenous structure, indistinct margins, an increased density of the surrounding fatty tissue indicated the presence of reactive changes, which could be consistent with hyperplasia or metaplastic lesion (Fig. 10).

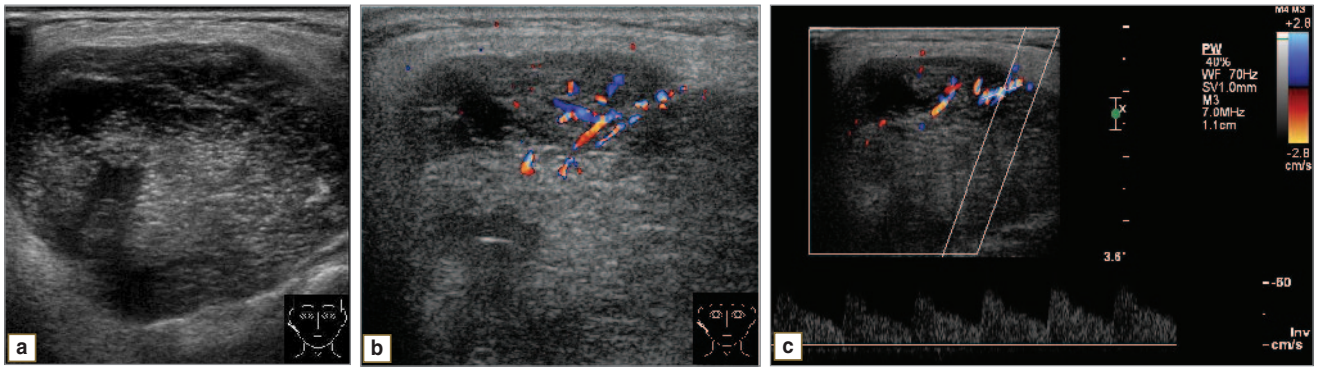

Fig. 9. Echogram of the right PSG: *a* — B-mode, a mass lesion with irregular contours, of sharply reduced echogenicity, heterogeneous structure; *b* — color Doppler mapping mode demonstrates numerous vessels in the tumor structure; *c* — pulse wave Doppler mode reveals high-speed arterial blood flow (over 60 cm/s)

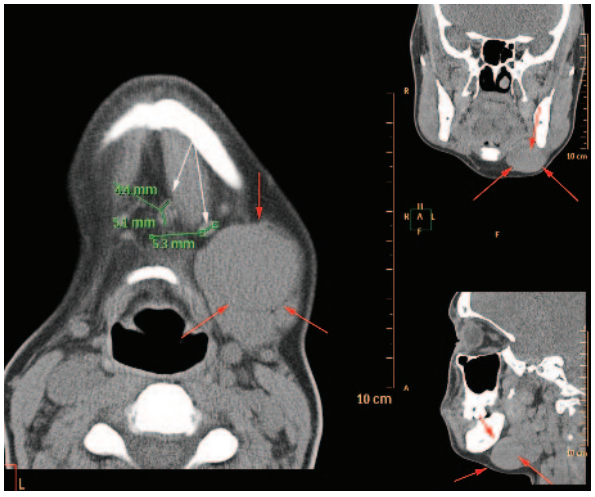

Fig. 10. Multidetector CT images (native investigation, multiplanar reconstruction) show the left SMSG to be enlarged due to a soft tissue mass (red arrows) surrounded by a thin-walled capsule, with irregular, occasionally indistinct contour. There are seen the change of oval-shaped regional lymph nodes (white arrows) with heterogeneous structure

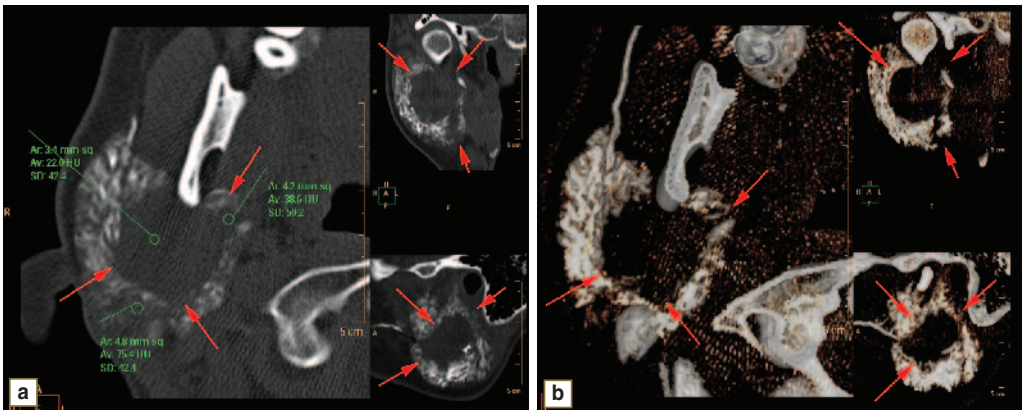

Fig. 11. Multidetector CT sialograms: *a* — multiplanar reconstructions; *b* — 3D-reconstructions show the tumor of heterogeneous density in the right PSG parenchyma (arrows), with irregular, indistinct margins. The tumor is manifested in the changes of the gland parenchyma, the deformity and discontinuity of the ducts

Multidetector CT sialography enabled to demonstrate more adequately the expansion of destructive changes in SG due to the tumor soft tissue proliferation in parenchyma. In all cases the ductal system was deformed, displaced, there were observed discontinuity of the ducts. 3D-reconstructions enabled to improve the spatial perception of SG ductal system, assess topographo-anatomical characteristics of the tumor (Fig. 11, *a, b*).

The assessment of multidetector CT sialography efficiency in the diagnosis of tumor and tumor-like masses

were the following: sensitivity — 100%; specificity — 95.0%; accuracy — 97.0%; positive predictive value — 95.0%; negative predictive value — 100%.

Conclusion. High resolution ultrasound is the primary diagnostic technique of neoplastic processes of major salivary glands, and enables to evaluate reliably the mass localization, shape, size, structure, margins and blood supply level. Multidetector computer tomographic sialography using multiplanar and 3D-reconstructions enables to assess more precisely topographo-anatomical relations of tumors and tumor-like masses of salivary glands with duct system, adjacent osseous and soft tissue structures and makes it possible for a clinician to determine the management of the operative therapy.

References

1. *Algoritmy diagnostiki i lecheniya zlokachestvennykh novoobrazovaniy* [Diagnostic and treatment algorithms of malignant neoplasms]. Pod red. Chissova V.I. [Chissov V.I. (editor)]. Moscow: FGU "MNIOI im. P.A. Gertsena Minzdrava Rossii"; 2010; 543 p.

2. Solov'ev Yu.N. Opukholi kostey: klassifikatsiya, nomenklatura, problemy diagnostiki [Osseous growths: classification, nomenclature, diagnostic problems]. *Arh Patol — Pathology Archives* 2003; 5: 3–6.

3. Fedyaev I.M., Bayrikov I.M., Belova L.P., Shuvalova T.V. *Zlokachestvennye opukholi chelyustno-litsevoy oblasti* [Maxillo-facial malignant tumors]. Moskow–Nizhny Novgorod: Meditsinskaya kniga, Izd-vo NGMA; 2000; 160 p.

4. Vuytsik N.B., Butkevich A.Ts., Kuntsevich G.I., et al. Differentsial'naya diagnostika mezhdu ostrymi vospalitel'nymi i opukholevymi obrazovaniyami golovy i shei [Differential diagnostics between acute inflammatory and tumor masses of head and neck]. *Klin Med — Clinical Medicine* 2008; 1: 58–61.

5. Smyslenova M.V. Metodika ul'trazvukovogo issledovaniya bol'shikh slyunnykh zhelez [Ultrasound investigation technique of major salivary glands]. *Radiologiya – praktika — Radiology – practice* 2013; 2: 61–69.

6. Schade G. Use of Ensemble tissue harmonic imaging to improve the resolution in ultrasound investigations of the head and neck area. *Laryngorhinootol* 2002; 81(6): 413–417.